JOURNAL OF APPLIED POLYMER SCIENCE VOL. 20, 2921-2940 (1976)

Some Structural Aspects of Sisal Fibers

B. C. BARKAKATY,* *Textile Physics Laboratory, Department of Textile Industries, The University, Leeds, LS2 9JT, England*

Synopsis

A critical account has been presented of the recent investigation on the chemical modification of lignocellulosic sisal fibers. The molecular structure of the paracrystalline cellulose, which forms the major constituent of the fiber, was studied by x-ray diffraction technique. Scanning electron microscope examination of the multicellular structure, surface topology, and fracture morphology of the fiber was carried out. The mechanical properties of the sisal ultimate cell and the "technical" fiber have been investigated by means of a microextensometer and an Instron tensile tester, respectively.

INTRODUCTION

Sisal belongs to the Agave family (Agave = Greek, noble), a plant group which produces long leaves from which the commercial fibers are extracted. It is grouped under the broad heading of the "hard fibers," among which sisal is placed second to manila in durability and strength.[1]

The long vegetable fibers constitute almost 20% of the total world production of industrial fibers.[2] While the major percentage of hard fibers is utilized in the manufacture of agricultural twines, with increased production of sisal in the recent years its commercial use has been successfully diversified.[3]

The use of sisal as a textile fiber by mankind can be traced back to antiquity.[1] Along with the study of agronomic and industrial aspects, a thorough fundamental investigation on the sisal fiber was carried out by Wilson.[4] He also paid detailed attention to the possibility of chemically modifying the fiber and put forward arguments for rejecting the idea due to the sacrifices that have to be allowed for the loss in strength, etc., as a result of chemical treatments.

In view of the escalating cost of production of the highly competitive man-made fibers, the natural long vegetable fibers of commerce today deserve much attention for further research aimed at the diversification of their potential end use. With this aim in view, investigation has been carried out on the structural and mechanical properties of untreated and chemically modified sisal fibers, which provides a background for the behavior of the fiber toward the action of chemical reagents used to bring about modification in their physicochemical properties.

* Present address: Faculty of Education, University of Khartoum, Khartoum, Sudan.

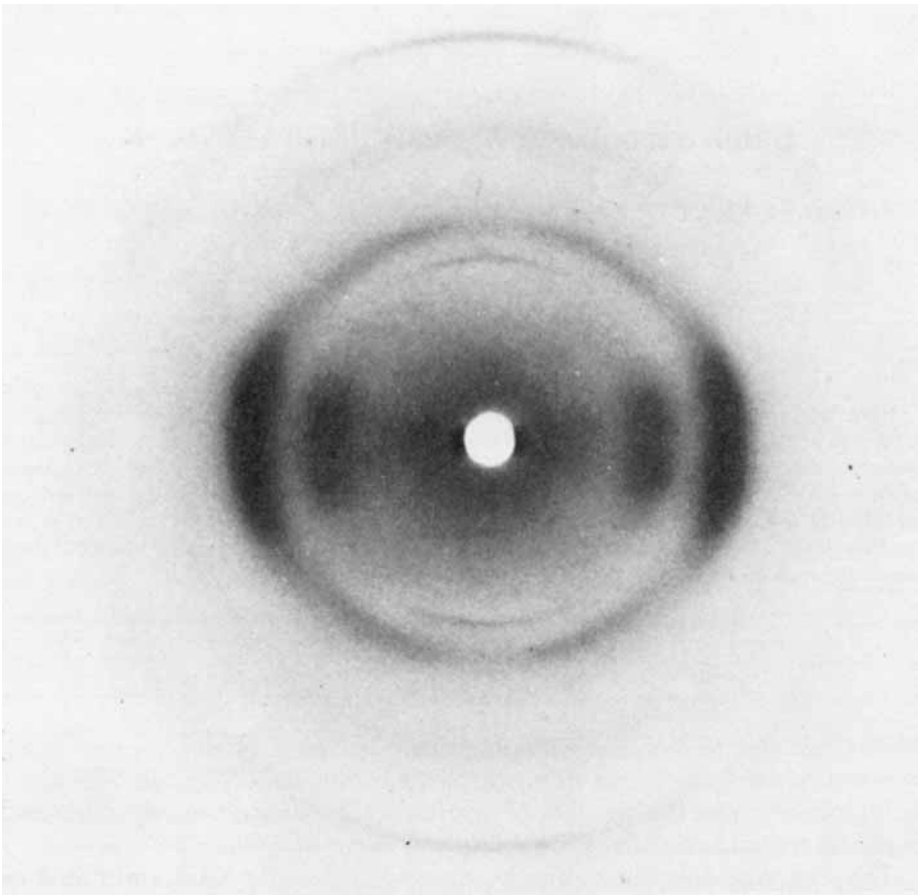

Fig. 1. X-Ray photograph of natural sisal fibers.

EXPERIMENTAL

Materials and Methods

Sisal fibers were dewaxed by Soxhlet extraction for 24 hr using a mixture of benzene and alcohol (1:1). After thorough washing with distilled water, the sample was dried in air.

The single ultimate cells (building units of a technical fiber) were obtained by alternate treatments in acidified (with excess concentrated hydrochloric acid) sodium hypochlorite and 3% hot sodium sulfite solutions.[5] The aggregates of the fiber ultimates were repeatedly washed in distilled water and air dried.

The samples for the examination in the scanning electron microscope (SEM) were coated with silver, by evaporation *in vacuo*, since only this method reveals the finest details of the surface topography.[6]

Molecular Structure by X-Ray Diffraction

Cellulose forms about 78% of the chemical composition of the sisal fiber, with 8% lignin, 10% hemicelluloses and pectins, 2% waxes, and 1% ash con-

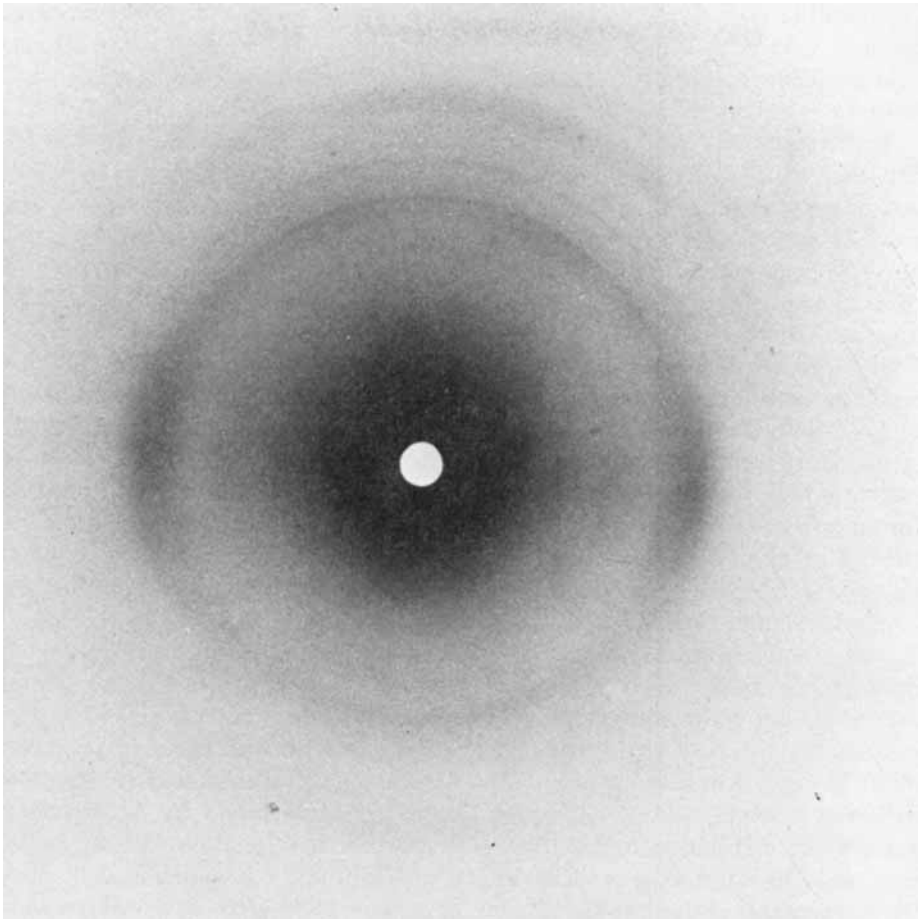

Fig. 2. X-Ray photograph of sisal fibers treated with 2% H_2SO_4 and 18% NaOH.

tent.[4] All natural long vegetable fibers are composed of ultimate cells which are bound together by a cementing material, mostly thought of as lignin. The dimensional variability is enormous among the ultimates from the same fiber as well as those from different fibers. Mukherjee and Radhakrishnan[2] have described the fineness variation of the ultimates as according to their location in the plant, stem, stalk, or leaf as well as on the degree of splitting ("disaggregation") of the entangled mass.

The x-ray diffraction technique was used to assess the molecular structure of the ordered regions of the fiber. In agreement with reported work on other lignocellulosic vegetable fibers,[7,8] the x-ray photograph of the natural sisal fiber is essentially due to a crystalline lattice of cellulose I, with a prominent diffuse background (Fig. 1). Mukherjee and Woods[9,10] investigated the behavior of the (101) and (10$\bar{1}$) spacings in jute and sisal, both in the natural and mercerized conditions, and concluded that the transformation to cellulose II is *mostly* partial, but under certain humidity conditions it may be complete. While majority of the research workers in the ligneous textile fibers[2,11] share the former view of the above authors, the latter conclusion needs further analysis. In the present experiments for sisal, the resolution of

(101) and (10$\bar{1}$) reflections was poor, in conformity with other works reported for jute. As in the case of other cellulosic fibers studied with x-ray diffraction techniques, the intensities of (020) reflections were greater than those of (040) (cf. electron diffraction technique[12]).

Treatments of Soxhleted sisal samples with aqueous sodium hydroxide solutions of different concentrations (9, 18 and 28%, respectively) in the *slack* condition were carried out at room temperature. The former two concentrations (reaction time 1 hr) did not show any changes in the lattice structure, whereas treatment in 28% solution of sodium hydroxide (reaction time 15 min) showed changes in the degree of crystallinity and orientation, with no apparent change in the cellulose I lattice.

Since it was mentioned[8] that modification to cellulose II of jute cellulose could be brought about only by a pretreatment with 2% sulfuric acid solution at boil, before immersion into a sodium hydroxide solution of mercerizing strength, the experiment was carried out for sisal. Lattice modification to cellulose II was obtained by treating sisal fibers with 2% sulfuric acid solution for 40 min at boil, followed by a treatment with 18% sodium hydroxide solution (1 hr at room temperature, henceforward to be referred to as a "combined treatment"). The above result is the *first* to be obtained in the study of chemical modification of sisal (Fig. 2).

The effect of mineral acids on cellulosic materials is, in general, to cause depolymerization resulting in short-chained fragments. The x-ray photograph did not show any evidence of the breakdown of the cellulose I lattice pattern for the sisal fibers which had undergone the sulfuric acid pretreatment alone. A detailed study of the treatment of sulfuric acid solutions of different concentrations, with jute fibers was undertaken by Mukherjee[13] using x-ray diffraction technique. He reported that "acid mercerization" of jute could be effected at an acid concentration of 950 g/l., which is well above the concentration used at the present experiment (36 g/l.). Sisal fibers were found to be in the fibrous form, after removing acid and air drying. Our conclusion that the x-ray photograph was that of native cellulose I, after acid pretreatment, is in agreement with the above author. The microscopic examination of the surface structure of the pretreated fibers show fibrillation—an effect due to the "intracrystallite" swelling by the acid[13] which, we believe, facilitates subsequent penetration of the sodium hydroxide solution, bringing about modification to cellulose II. This result supports the view of Sen and Woods[14] that, although the location of lignin in a vegetable fiber is mostly "extracrystalline," there may be some lignin content in the "crystalline–amorphous" boundaries with an effective influence in the crystalline regions.

Various authors investigated the behavior of jute fiber during and after treatment with sodium hydroxide solution. Saha[15] published the graphic representation of the mercerizing behavior of jute along the line of Sisson and Saner[16] for cotton cellulose, at different temperatures (−10°C to 60°C), and with varying concentrations of alkali (5 to 50%). Sirker and Saha,[17] however, showed that the structure obtained for jute fiber, after treatment with 30% sodium hydroxide solution, was a new modification, different from that of water cellulose or ordinary hydrated cellulose. Mukherjee[13] also stated that the "acid mercerized" structure of jute might be a different polymorphic

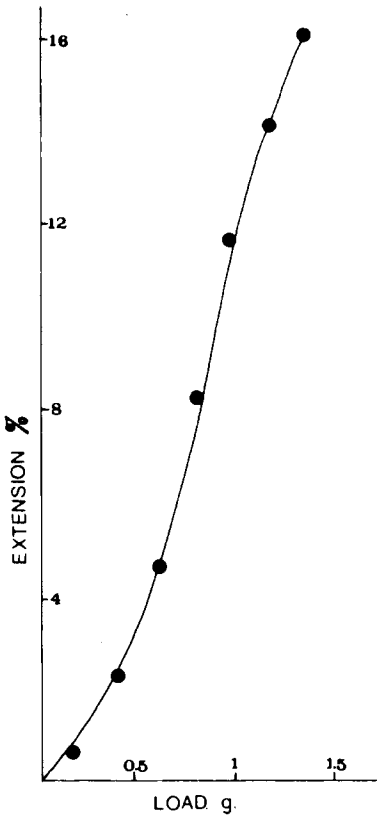

Fig. 3. Tensile properties of sisal ultimates.

transition of the native cellulose. Sen and Woods,[14] however, challenged the above proposal of Sirker and Saha and showed that a 20% solution of alkali at 20°C brought about transformation to cellulose II in jute. By progressive lowering of the moisture content, Mukherjee and Woods[9] showed that cellulose II lattice structure was obtained for ramie, jute, and sisal and manifested itself in the continuous decrease of the (101) x-ray diffraction spacings. They went on to comment that the degree of readjustment in the molecular structure in the case of jute and sisal lags behind that in ramie. The above circumvents their earlier arguments that the location of some of the "disturbing" component lignin, near the boundaries of the crystallites, is preventing the penetration of water molecules or chemical agents.

A direct comparison of our present results of the molecular transition to cellulose II, observed in the case of sisal under the combined treatment, with that of Mukherjee and Woods[9] cannot, however, be made because of different experimental conditions. It is, therefore, concluded that a transition to cellulose II lattice in sisal fibers can be achieved by the combined (acid + alkali) treatment. Moreover, treatment with sodium hydroxide solutions alone does not produce a mixed-type crystallization (cellulose I + II) as suggested by some authors[7,8,11] in the case of jute and banana fiber. Since crystalline transition has been obtained in the combined treatment under optimum con-

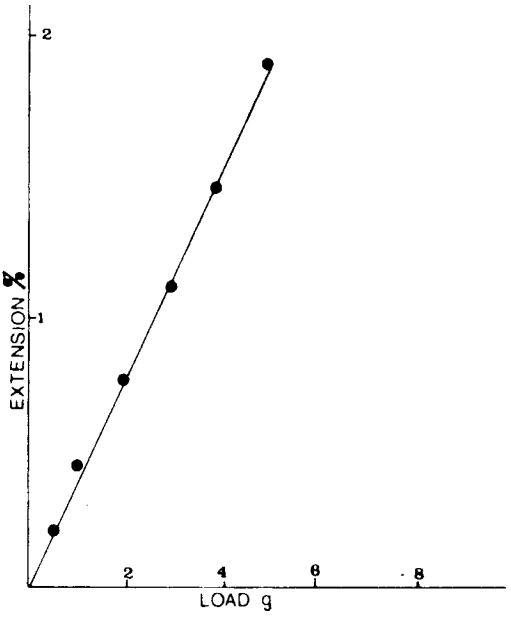

Fig. 4. Tensile properties of sisal ultimates.

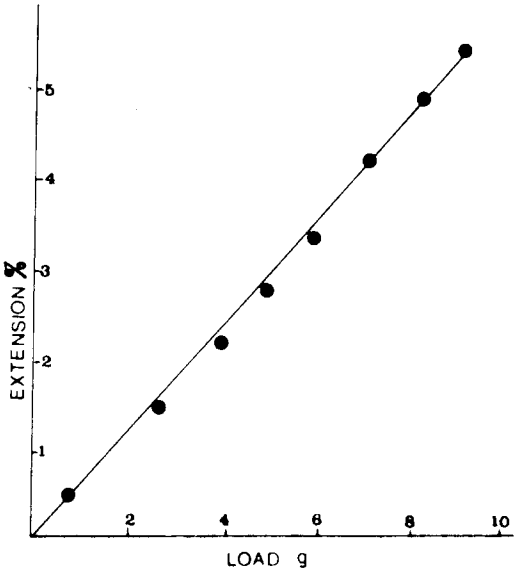

Fig. 5. Tensile properties of sisal ultimates.

ditions, it must be pointed out that any such intracellular transformation is only reflected in the gross technical fiber providing the intracellular cohesion remains unimpaired.[4]

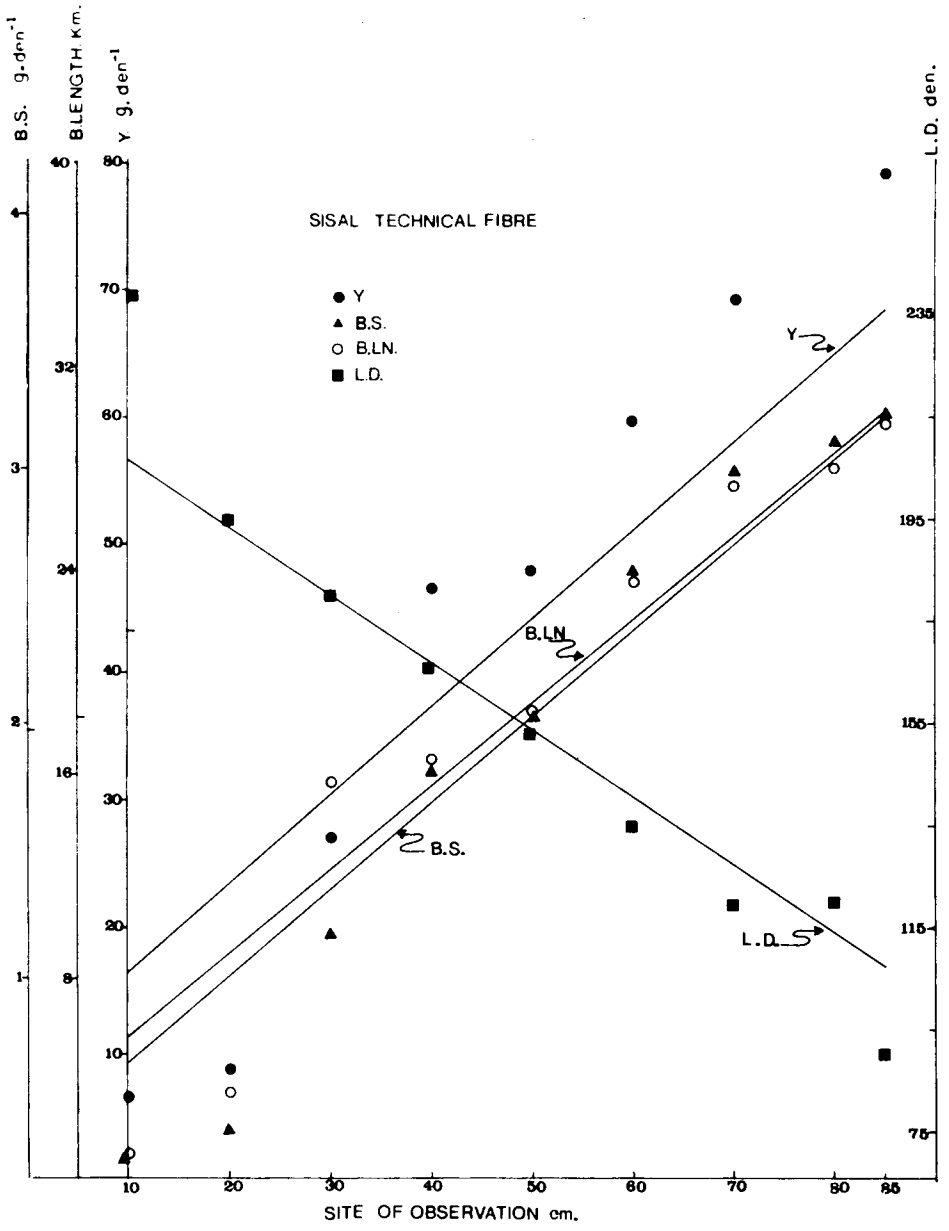

Fig. 6. Mechanical parameters at different sites of observation along length of the sisal fiber.

Tensile Properties of Sisal Single Cells

The load–extension curves of sisal ultimates (described under Materials) were obtained by means of a microextensometer[5] which incorporated a sensitive proximity meter coupled to a chart recorder. The ultimate cells were mounted in a special mounting device, using Durofix as adhesive. When transferred to the clamping positions of the instrument, one part of the mount is screwed onto a movable beam attached to one plate of the condenser

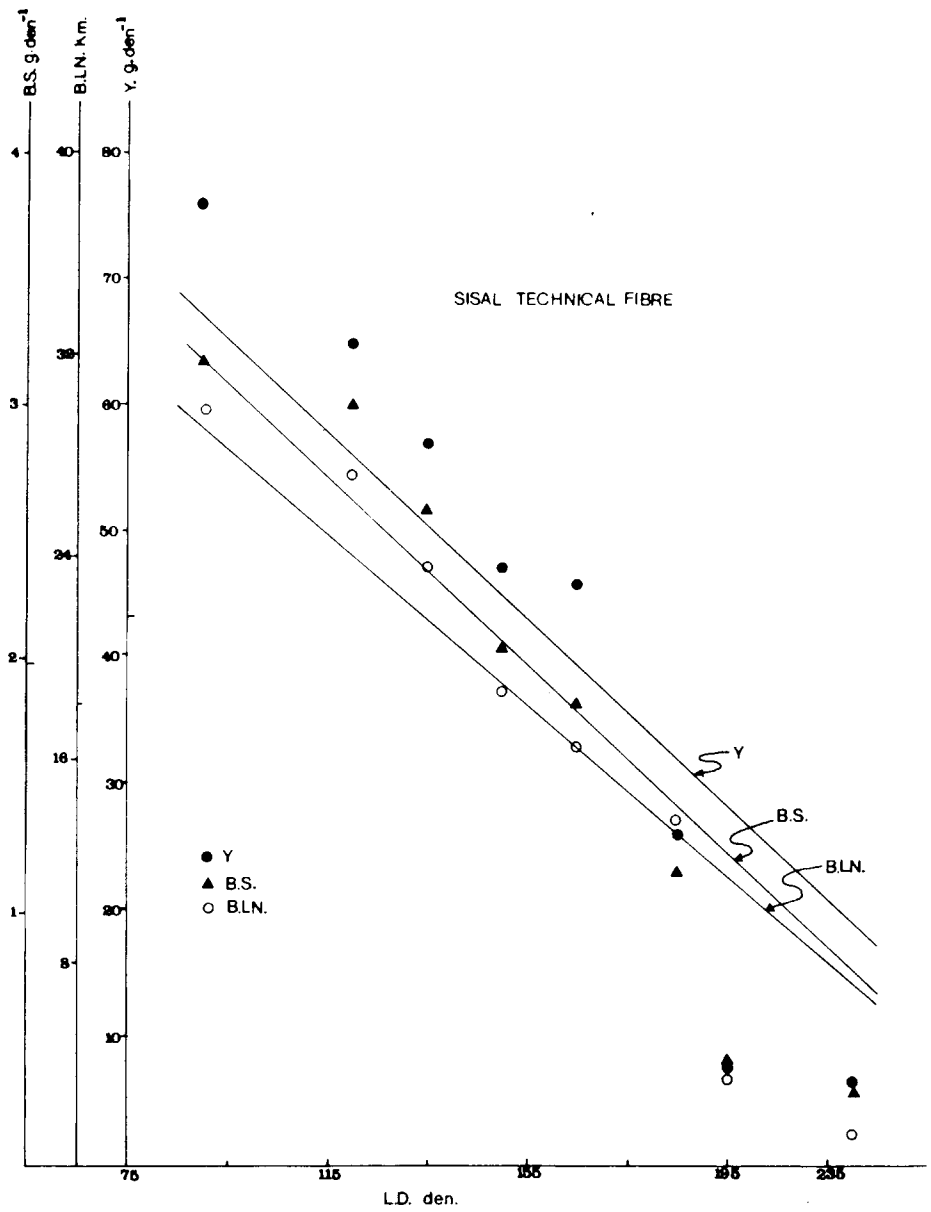

Fig. 7. Variation of mechanical parameter with linear density of sisal fibers.

and the other, to a fixed support. Until the beam is let free under zero load, the ultimate cell was held clamped in the device. The results obtained showed that there were two distinct types of ultimate cells characterized by their extensibility. These results are in agreement with published data[5] which show that the "low modulus" fiber cells originate from the butt end, whereas the "high modulus" cells from the tip end of the technical fibers (Figs. 3 and 4). The load–extension relation for a bundle of ultimate cells, as expected, illustrates the dependence of tensile properties of the sisal fiber on the mode of assembly of ultimate cells (Fig. 5).

Mechanical Properties of the Untreated Fibers

The tensile parameters, namely, (i) breaking length, (ii) breaking stress, (iii) breaking load, (iv) breaking extension, and (v) Young's modulus of a technical fiber at different positions along the length, were determined by using an Instron tensile tester. The adopted procedure was to chop a bundle of commercial fiber, about 85 cm long, into 10-cm sections from the ends of which the samples were selected. The technical fibers were mounted onto the paper frames, using Durofix as adhesive. Approximately 15 to 20 samples of experimental length 2 cm were tested for each position of observation. The regression lines of the mechanical parameters, obtained from the load–elongation curves, were plotted to elucidate the relation between them on one hand and the site of observation or the linear density (denier) on the other.

Breaking stress, breaking length, and Young's modulus were found to increase linearly along the length from the base to the tip end of the technical fiber (Fig. 6). Since the linear density is a decreasing function of the site of observation (Fig. 6), the above mechanical parameters are an inverse function of the linear density (Fig. 7).

The results agree with the suggestion that the tensile properties of sisal depend on the microfibrillar orientation in the secondary wall of the plant cell. Experimental demonstration of the above property has been made in the case of textile fibers by Meredith,[18] Balashov et al.,[19] and Spark et al.[5] The general conclusion is that the smaller the spiral angle, the greater is the strength of the fiber. Although Balashov and others showed that, when sisal fibers were extended, the x-ray photograph revealed a decrease in the spiral angle, Chakravarty and Hearle,[20] working on nine different plant fibers including sisal, conveniently *assumed* a mean spiral angle of approximately 23° for sisal

TABLE I
Chemically Treated Sisal Technical Fibers[a]

Sisal treated with	B.L., g	B.E., %	B.S., g/den^{-1}	B. Length, km	Y, g/den
1. 9% NaOH (1 hr at 20°C)	229.2	2.93	2.524	22.72	80.61
2. 18% NaOH (1 hr at 20°C)	420.0	3.77	4.888	43.99	129.65
3. 28% NaOH (2 min at 20°C)	232.7	2.22	3.879	34.91	174.72
4. 28% NaOH (15 min at 20°C)	192.2	3.55	3.204	28.84	90.25
5. 2% H_2SO_4 (40 min at boil)	41.9	1.22	0.699	6.291	57.29
6. 2% H_2SO_4 (40 min at boil) + 9% NaOH (1 hr at 20°C)	31.9	1.76	1.063	9.567	60.39
7. 2% H_2SO_4 (40 min at boil) + 18% NaOH (1 hr at 20°C)	91.6	4.92	3.038	27.34	61.74

[a] Sample length = 2 cm; cross-head speed = 1 cm/min; chart speed = 50 cm/min; B.L. = breaking load: B.E. = breaking extension; B.S. = breaking stress; B. Length = breaking length; Y = Young's modulus.

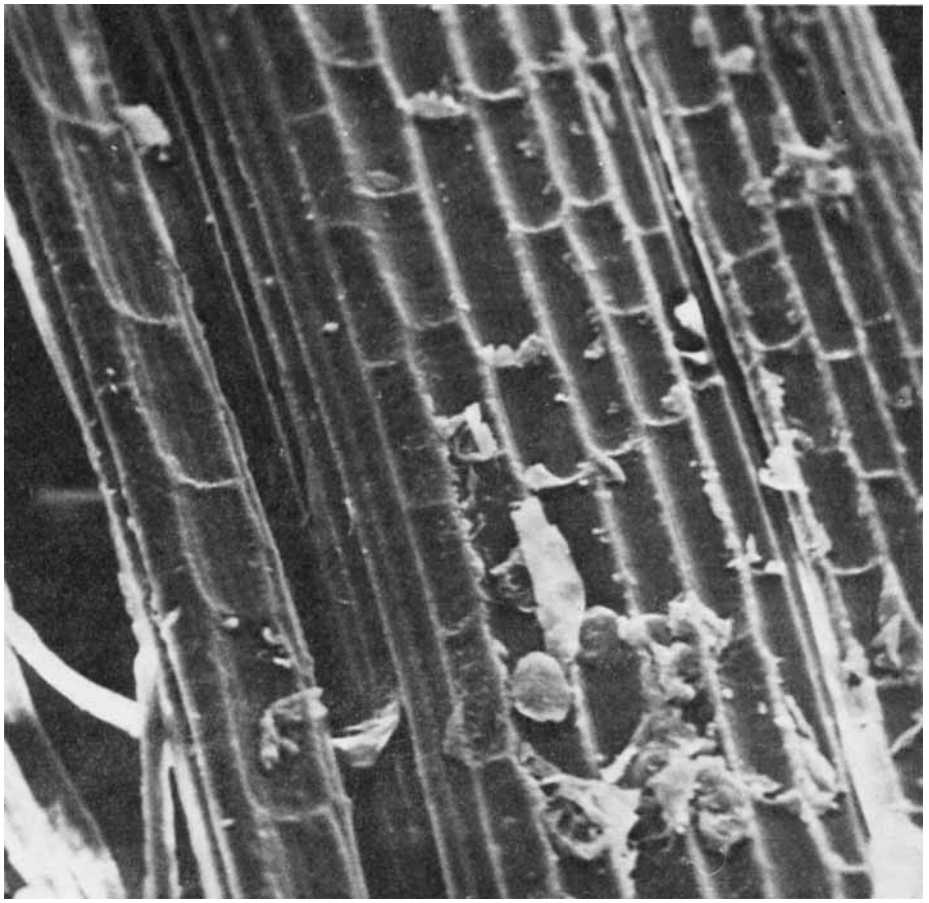

Fig. 8. Surface structure of raw sisal fibers.

and aloe fibers and concluded that the extension of such fibers was the result of stretching of the microfibrils and not due to a helical "spring action" as demonstrated by Stern[21] and later accepted by Jarman et al.[22] for the coir fiber.

The present experimental results are in accord with the idea that the spiral angle decreases linearly from the butt to the tip end of sisal fibers. They are, however, at variance with the conclusion arrived at by Wilson[4] who showed that above about 28 cm from the butt end, the breaking length remains almost constant (ca. 42 km). Lock,[3] in his monograph on sisal, viewed Wilson's data with reservation and commented that "single fibre strength tests are by no means absolute, they are subject to a considerable margin of error due to the variable nature of the fibre." He concluded that the average strength of the fiber increases with the age of the plant, which in turn reflects that short fibers are weaker than the long ones and that strength increases from the base to the tip of an individual fiber. He also reported different values of breaking length of sisal fibers of different origin. The differences in the results on the measurement of mechanical properties of a single fiber due to commercial processing and storage cannot, however, be ruled out.

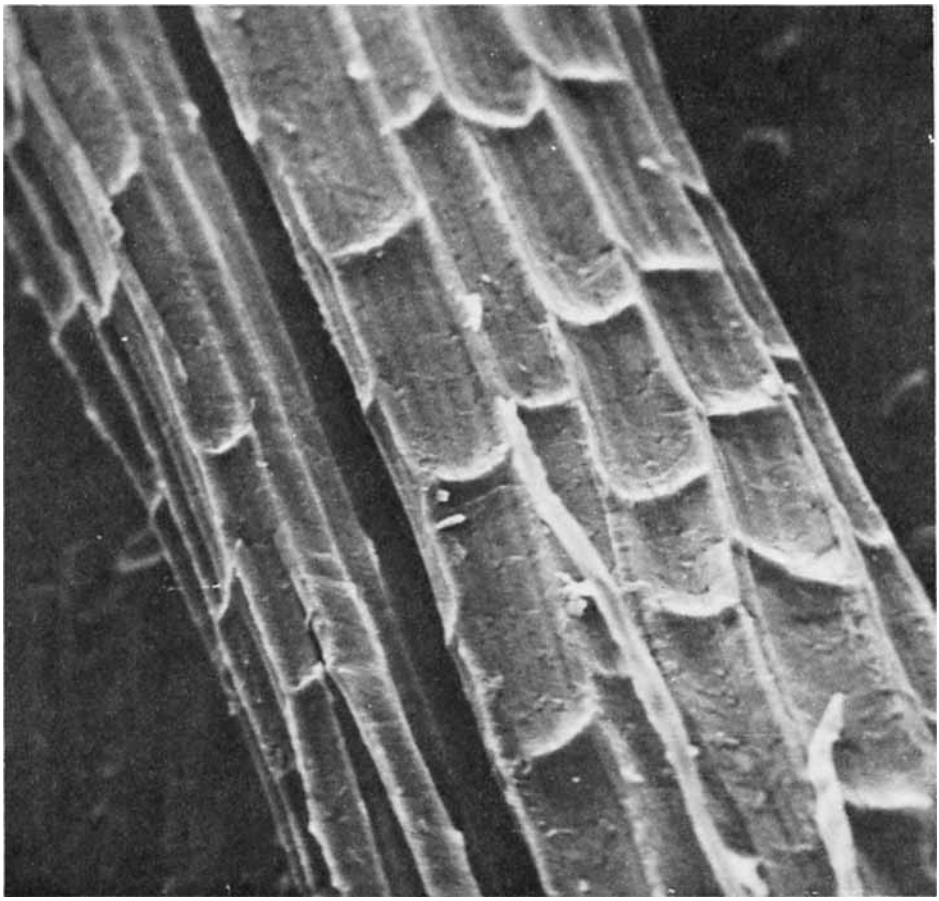

Fig. 9. Surface structure of delignified sisal fibers.

Since the test lengths were different for experiments with sisal ultimate cells and the technical fiber, a direct comparison of the tensile properties between the two sets of results should not be pressed too far. As other experimenters[20] showed that the fiber ultimates have a greater extensibility and a lower initial modulus than a technical fiber, it can be argued that lignin and other noncellulosic substances modify the tensile properties of a vegetable fiber.

Mechanical Properties of the Chemically Modified Fibers

The mechanical parameters obtained from the load–extension curves of the chemically modified samples, selected at random, are presented in Table I.

Since the average breaking load for the untreated fiber was found to be 273 g, it is apparent that the load required to break is lower for all the chemically treated samples, except for the sample treated with 18% sodium hydroxide solution. Of particular interest are the reactions with (i) 18% sodium hydroxide, and (ii) 2% sulfuric acid solutions. With the former treatment, a great increase in strength, and with the latter, a great loss in strength were

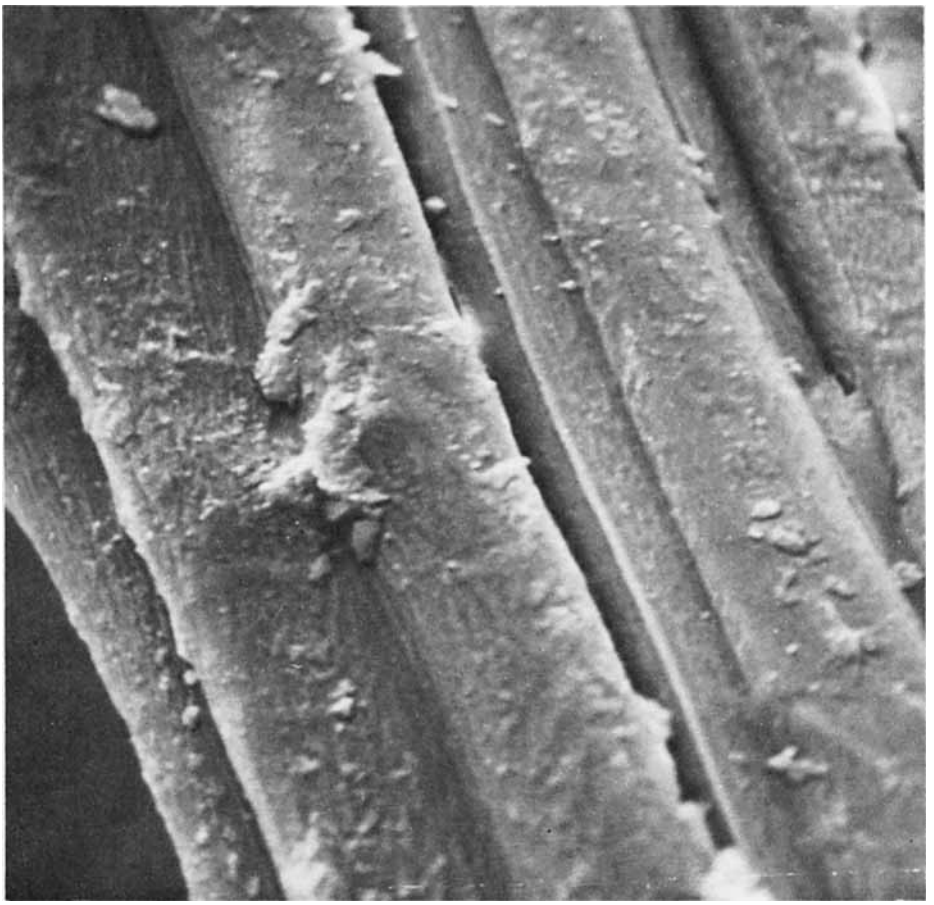

Fig. 10. Surface structure of 28% NaOH-treated sisal fibers.

obtained. After-treatment of the sulfuric acid-treated sample with increased concentrations of sodium hydroxide solutions increased the strength of the fiber, compared to the sulfuric acid-pretreated sample. Further, it has been observed that for the chemically modified samples break occurs simultaneously at several sections along the technical fiber, signifying that "drafting" of the ultimates has taken place as a result of the chemical reaction. The above conclusion agrees with the observation made by Chakravarty[23] in the case of jute fibers treated with 18% sodium hydroxide solution, where he found the fibers to break "with a succession of partial slippages." It is believed, therefore, that not only is there a loss in weight of the sisal fibers due to the effect of swelling agents as was shown by Wilson,[4] but also there is a concomitant tendency for the fiber ultimates to separate from the cementing "matrix." Such alkali treatments, however, do not impart technically viable properties to the fiber, which was also reasoned by Wilson in his work on sisal.

Surface Morphology of Raw and Chemically Modified Sisal Fibers

The surface structure of sisal fibers, both treated and untreated, was briefly investigated by means of the scanning electron microscope. The surface

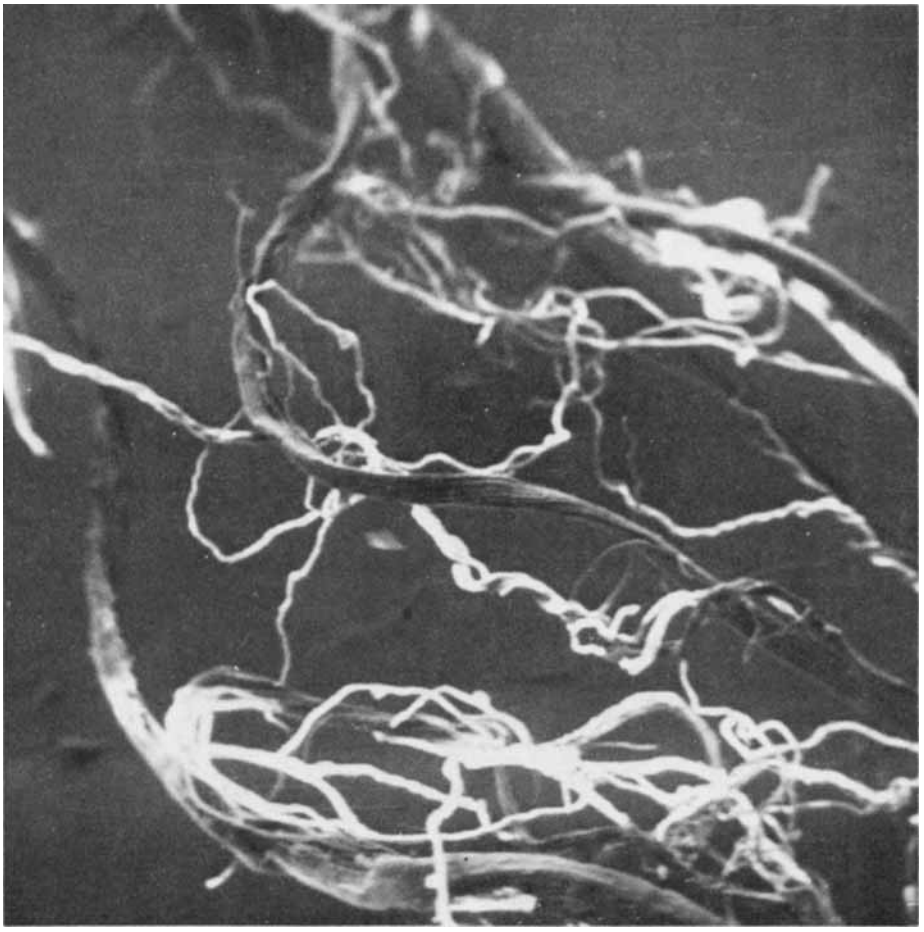

Fig. 11. Twisted structure in the combined treatment of sisal.

structures of the raw and partially delignified fibers are shown in Figures 8 and 9, respectively. The surfaces are marked, in both cases, by their characteristic vestigal attachments of the parenchymatous cells in which the fiber is embedded in the leaf. No apparent changes in the surface morphology are visible in the partially delignified fiber. The treatment with 28% sodium hydroxide solution (1 hr at 27°C) caused the fiber to fibrillate into the ultimates, so that their primary walls revealing the low degree of orientation of the fibrils could be observed (Fig. 10). Although the ultimate fibrillation and exposure of the primary wall could be seen for the fibers treated with 2% sulfuric acid solution (40 min at boil), the effect of the combined treatment (Materials and Methods section) on the surface morphology of the fiber is remarkable. The result of the combined treatment caused the fibers to twist (Fig. 11) as well as to undergo very high degree of fibrillation (Fig. 12). The fibrils on the surface of the ultimates are oriented almost parallel to the fiber axis. The same chemical reagents at room temperature (each treatment for 30 min) produced a lower degree of fibrillation, with a varying degree of orientation of the fibrils on the surface of the ultimate cells. As expected, better separation of the ultimates was observed with increasing temperature.

The surface morphology of the sisal ultimate cell obtained by the chemical

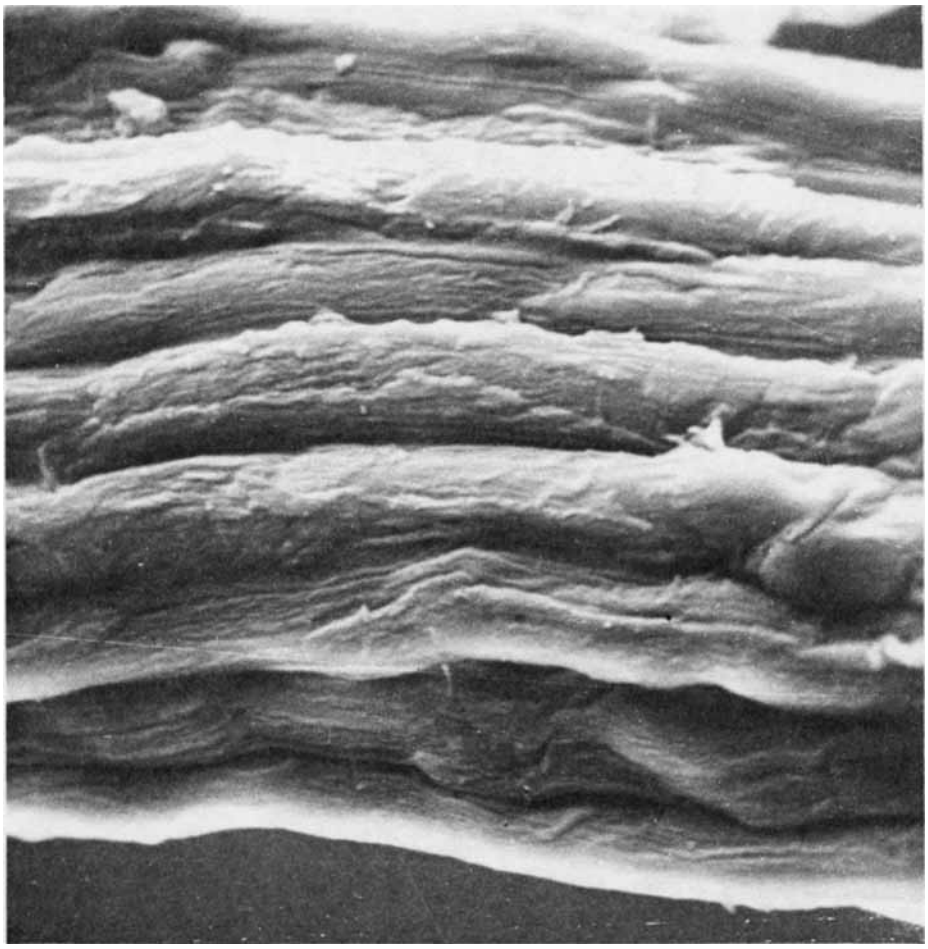

Fig. 12

disintegration process described in above is shown in Figure 13. It is tentatively suggested that the primary wall has been removed from some of the ultimates during the fragmentation process, causing the exposure of the oriented fibrils on the surface of the secondary wall. The sisal ultimates were further subjected to mechanodegradation by exposing to ultrasonic radiation for 4 hr in water medium. The fragments obtained showed markedly blunt ends, which does not agree with the general conclusion that the ultimates have tapered ends. This is presumably due to the breakage of the ultimates during ultrasonic irradiation. As shown in Figure 14, the diameter of the fragments varies remarkably from one fragment to the other, and within individual fragments along their lengths. Moreover, a right-handed twist (Z-twist) is apparent in most of the fragments of the aggregate under examination. Further removal of the primary walls from the ultimates which were not removed in the chemical disintegration process takes place. The remnants of the primary wall can be seen as featureless thin "flakes" in the elec-

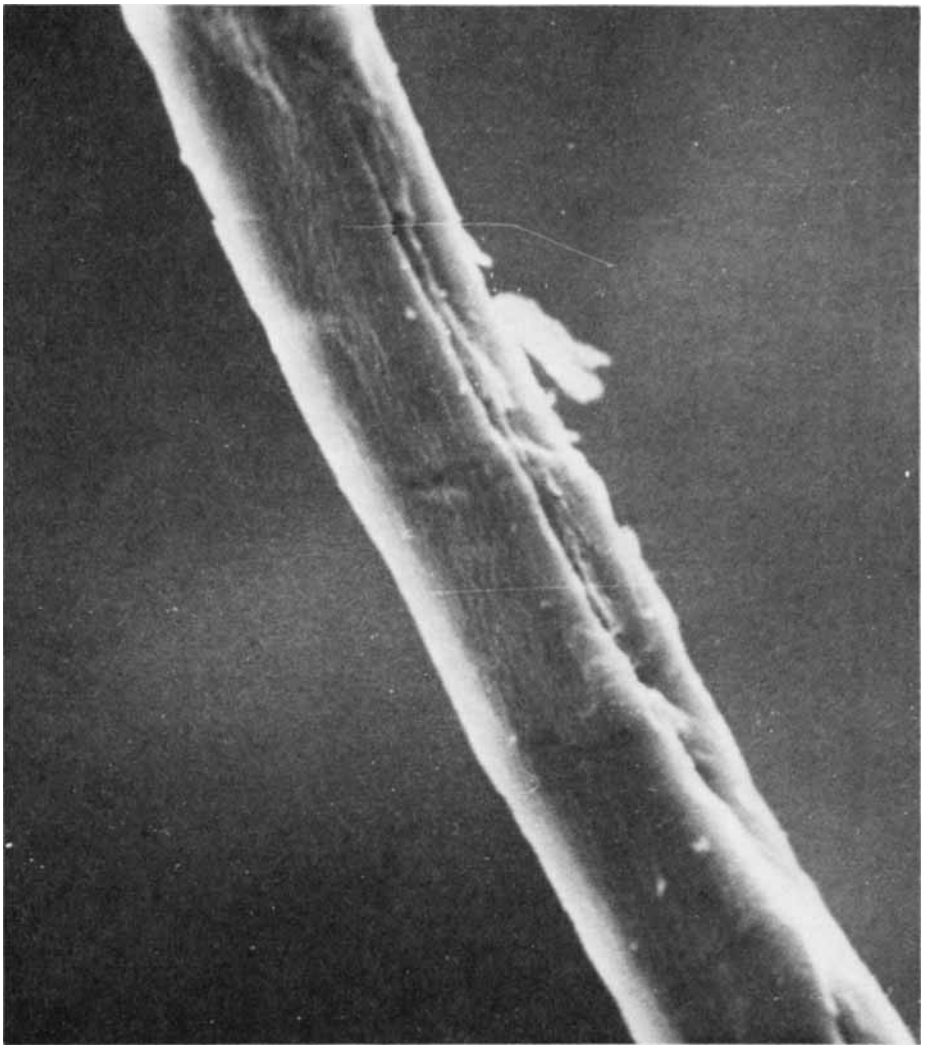

Fig. 13. Sisal ultimate cell produced by chemical treatments.

tron micrograph (Fig. 15). This type of removal of the primary wall from the surface of the ultimates of coir fiber, by ultrasonic disintegration was shown by Jarman and Laws[22] using an optical microscope. The fibrillar orientation of the sisal ultimates in the wall surface exposed during ultrasonic irradiation was mostly parallel to the fiber axis. In this mechanochemical phenomenon, the breakage of the fibrils which appears as "cracks" on the ultimate surface can also be observed.

The salient features of the fracture morphology of the sisal single cells, when stretched in air in the microextensometer, as revealed by the electron micrographs, are (i) the splitting into individual ultimates for a bundle of cells (Fig. 16) and (ii) a markedly concave surface at the fractured end of a single cell (Fig. 17). The latter type of fracture is accompanied by a stepwise breakdown of the cell wall, the fracture initiation being from the outer layer.

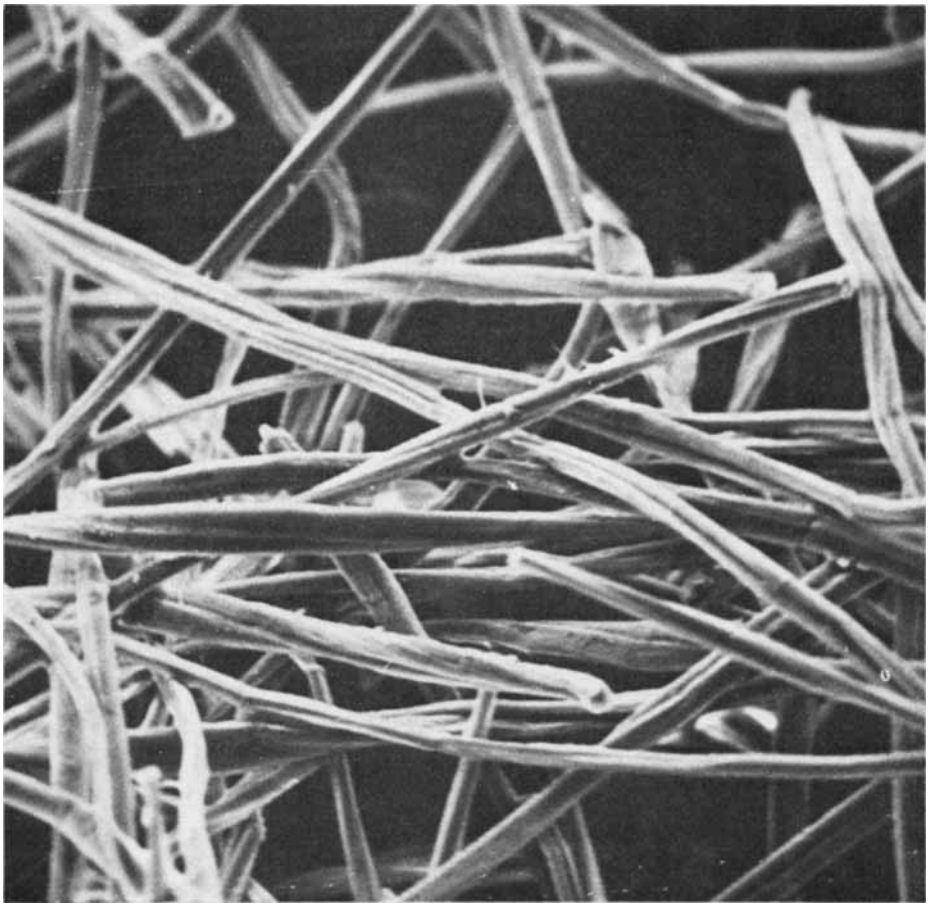

Fig. 14. Sisal ultimate cells subjected to ultrasonic radiation.

Further splitting into fibrils has not been observed.

The mode of fracture of a technical fiber, as can be visually observed during the Instron experiments, show both "green stick" and brittle fracture together with splitting into ultimates. The last type was found to be predominant in the chemically treated fibers. The importance of the study of fiber fractography has been aptly emphasized by Hearle and his associates[24] in a recent article in which the authors presented a classification of various types of fracture in natural and man-made fibers. They, however, pointed out that there are many variants and additions of the basic forms they observed which may be associated with (i) different types of fiber, (ii) previous history of the fiber, (iii) type of mechanical stress to which the fiber is subjected, and (iv) the medium (humidity) in which the fiber is fractured. A detailed examination of the modes of fracture of the sisal technical fiber by scanning electron microscope will be pursued in connection with further studies of the tensile behavior of the fiber.

Fig. 15. Sisal primary walls, appearing as "flakes" during ultrasonic disintegration.

The Multicellular Structure

The characteristic features of the cellular aggregates of a single technical fiber revealed in a transverse section under the scanning electron microscope are shown in the micrograph (Fig. 18). The size of the lumen is large compared to the secondary wall thickness. The middle lamellae and the (triangular) intercellular spacings can be easily observed. Breakage of the tertiary and, to a certain extent, the secondary wall can also be observed from the micrograph.

For one particular bundle of fiber, the lumen size was measured up to 25 cm from the base by a planimeter from the micrographs, which has been presented in Table II. While there is a gradual decrease in the lumen size from the base upward in that region, in good conformity with the "hollowness' measurement by Wilson[4] the large coefficient of variation shows the high de-

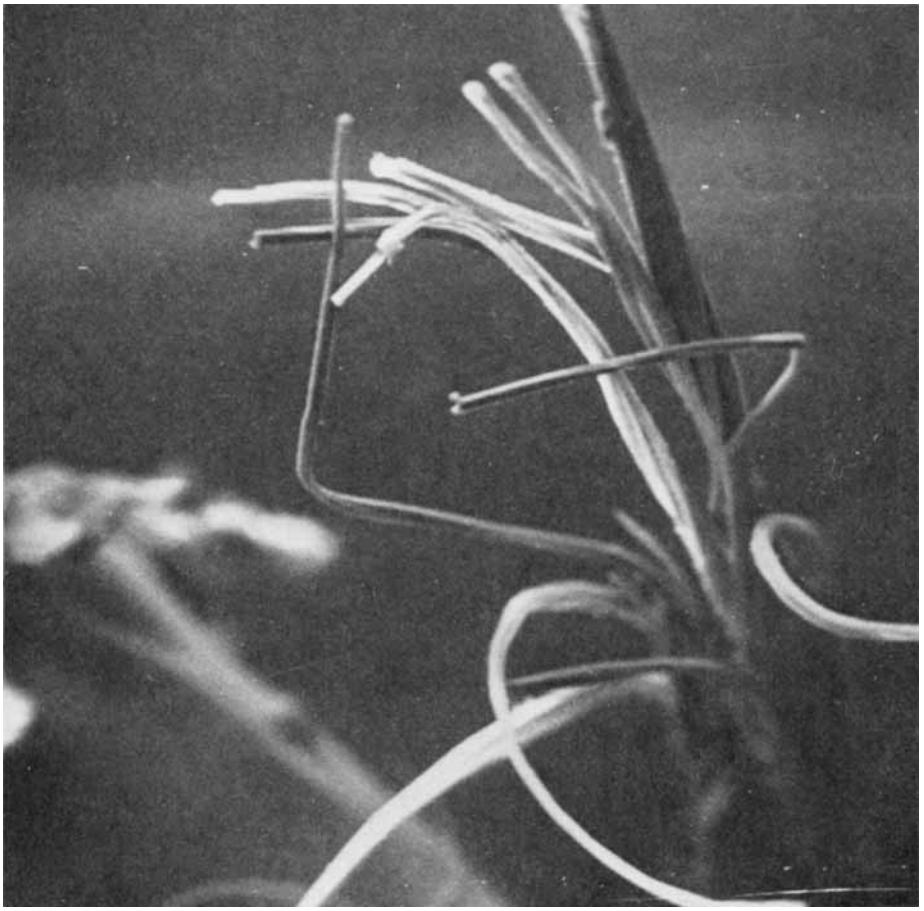

Fig. 16. Fracture of a bundle of sisal ultimates.

gree of variability of the size of the lumen at a particular cross-sectional position. This, in turn, exemplifies the variability in the size of the ultimates which form the technical fiber. Indeed, collapsed nature of the lumen was observed in certain fibers at some position along their length (which could not be generalized for all the fibers), doubtlessly being related to the particular event in the growth mechanism in the vegetative phase of the plant, during which the secondary wall thickening makes the lumen vanishingly small. Wilson demonstrated that the strength characteristics of the fiber can also vary due to the imperfect growth of the cell wall. It is, therefore, evident that the lumen in the fibrous cells plays the main role, among other factors, in determining the tensile and sorption behavior of the sisal fiber.

DISCUSSION

The study of the structural, mechanical, and fractural aspects of a fiber is at the grass roots in understanding its behavior during chemical and industrial processing. The present experimental investigation of the sisal fiber has offered an insight into the multicellular structure and the relation between the molecular structure and the mechanical properties of the fiber.

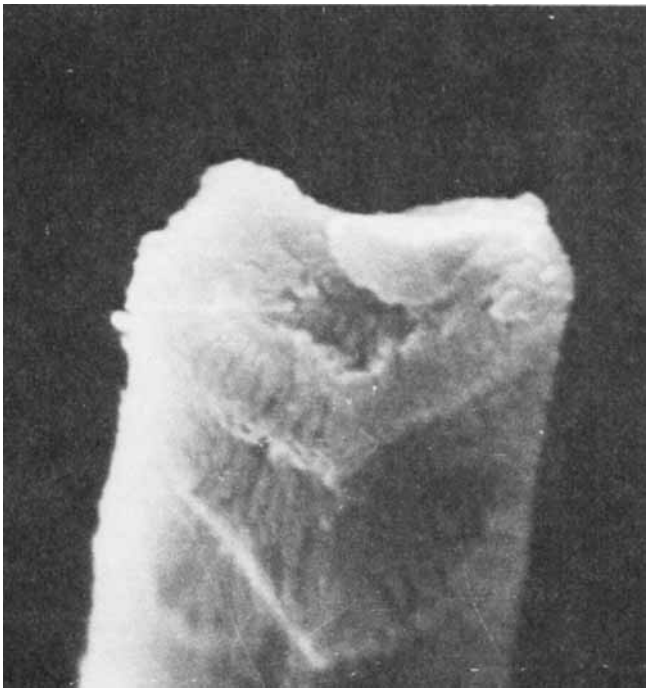

Fig. 17. Fractured end of a sisal single cell.

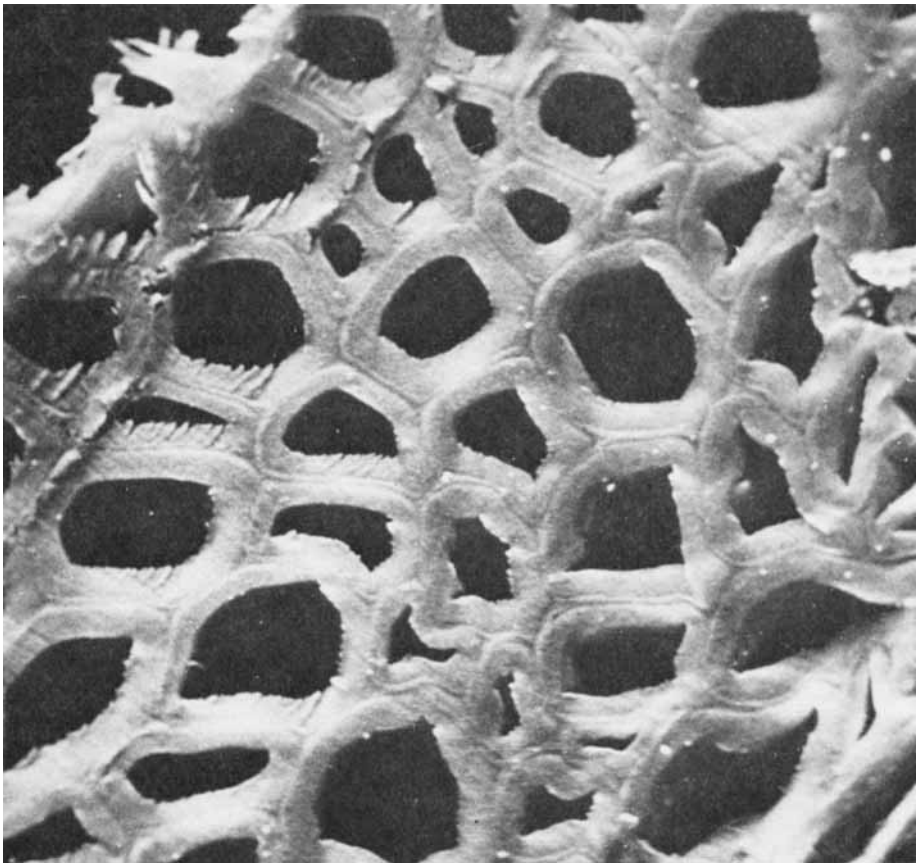

Fig. 18. Multicellular structure of sisal.

TABLE II
Measurement of Average Size of the Lumen in the Basal Region of the Sisal Fiber

Site of observation from the base, cm	Average area $\times 10^{-8}$, cm^2	Number of lumens measured	Coefficient of variation, %
10	113.6	12	56.0
20	49.6	20	65.6
21	12.9	19	51.8
24	9.6	14	50.0
25	4.8	9	13.3

The author wishes to acknowledge gratefully the award of a Postdoctoral Fellowship from the Tropical Products Institute, London, and his indebtedness to Dr. J. Sikorski for his continuous advice throughout all stages of this work.

References

1. L. Weindling, *Long Vegetable Fibers*, Columbia University Press, New York, 1947.
2. R. R. Mukherjee and T. Radhakrishnan, *Text. Progr.*, **4**, 4 (1972).
3. G. W. Lock, *Sisal*, Tanganyika Sisal Growers' Association, Longmans, London, 1962.
4. P. I. Wilson, *Sisal*, Vol. II, F.A.O., U.N.O., Rome, Hard Fibres Research Series, No. 8, April 30 1971.
5. L. C. Spark, G. Darnbrough, and R. D. Preston, *J. Text. Inst.*, **49**, T309 (1958).
6. S. Tolansky, *Vacuum*, **4**, 154 (1954).
7. M. K. Sen, Ph.D. Thesis, University of Leeds, United Kingdom, 1948.
8. R. R. Mukherjee, Ph.D. Thesis, University of Leeds, United Kingdom, 1949.
9. R. R. Mukherjee and H. J. Woods, *J. Text. Inst.*, **42**, T309 (1951).
10. R. R. Mukherjee and H. J. Woods, *J. Text. Inst.*, **41**, T422 (1950).
11. K. Venkateswarlu and K. Govindakutty Menon, *Acta Phys. Polon.*, **33**, 609 (1968).
12. L. D. Fernando, Ph.D. Thesis, University of Leeds, United Kingdom, 1974.
13. D. Mukherjee, Ph.D. Thesis, University of Leeds, United Kingdom, 1954.
14. M. K. Sen and H. J. Woods, *Nature*, **161**, 768 (1948).
15. N. N. Saha, *Indian J. Phys.*, **22**, 141 (1948).
16. W. A. Sisson and W. R. Saner, *J. Phys. Chem.*, **45**, 717 (1941).
17. S. C. Sirker and N. N. Saha, *Nature*, **157**, 839 (1946).
18. R. Meredith, *J. Text. Inst.*, **37**, T205 (1946).
19. V. Balashov, R. D. Preston, G. W. Ripley, and L. C. Spark, *Proc. Roy. Soc.*, **B146**, 460 (1957).
20. A. C. Chakravarty and J. W. S. Hearle, *J. Text. Inst.*, **58**, 651 (1967).
21. F. Stern, *J. Text. Inst.*, **48**, T21 (1957).
22. C. G. Jarman and V. Laws, *J. Roy. Micros. Soc.*, **84**, (Pt. 3), 339 (1965).
23. A. C. Chakravarty, *Indian J. Technol.*, **5**, 333 (1967).
24. J. W. S. Hearle, B. Lomas, and A. R. Bunsell, *Appl. Polym. Symp.*, **23**, 147 (1974).

Received June 4, 1975
Revised September 9, 1975